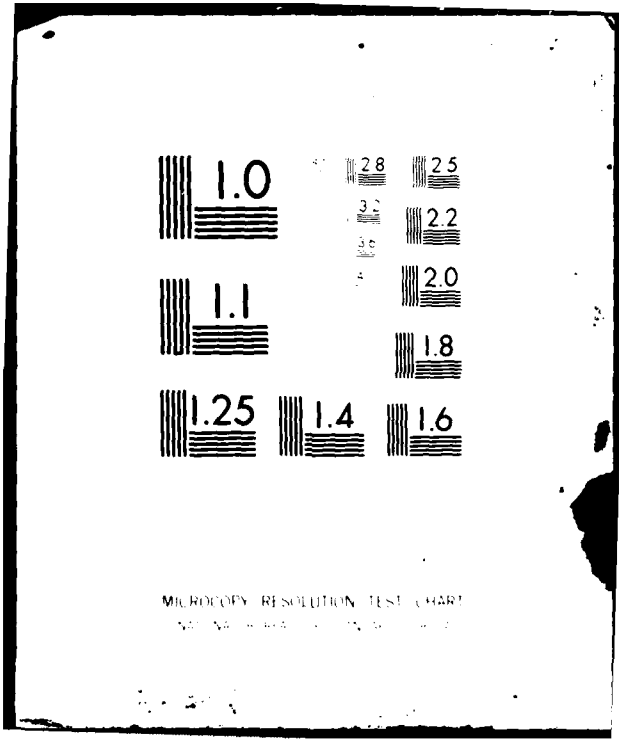


AD-A109 506 MASSACHUSETTS UNIV AMHERST DEPT OF POLYMER SCIENCE --ETC F/G 11/9  
FRACTURE AND INTERFACE STUDIES OF ARAMID REINFORCED POLYAMIDE C--ETC(U)  
UNCLASSIFIED OCT 81 S J DETERESA, R J FARRIS, R S PORTER N00014-75-C-0686  
TR-16 NL

1 of 1  
AL A  
COPY E

END
DATE
FORMED
02 82
DTIC



MICROCOPY RESOLUTION TEST CHART  
NATIONAL BUREAU OF STANDARDS-1963-A

**LEVEL**

(12)

AD A109506

OFFICE OF NAVAL RESEARCH

Contract No. N00014-75-C-0686

Project No. NR 356-584

TECHNICAL REPORT NO. 16

"FRACTURE AND INTERFACE STUDIES OF ARAMID REINFORCED  
POLYAMIDE COMPOSITES: COMPRESSIVE EFFECTS  
AND CRITICAL LENGTH MEASUREMENTS"

by

Steven J. DeTeresa, Richard J. Farris and Roger S. Porter  
Polymer Science and Engineering Department  
Materials Research Laboratory  
University of Massachusetts  
Amherst, Massachusetts 01003

October 20, 1981

SELECTED  
JAN 11 1982  
A D

Reproduction in whole or in part is permitted for  
any purpose of the United States Government

Approved for Public Release; Distribution Unlimited

DTIC FILE COPY

82 01 11 056



## INTRODUCTION

The increased use of fiber-reinforced composites to replace conventional materials has been motivated primarily by weight savings. While epoxy with carbon or glass fiber systems are the most extensively used and studied, alternatives can be found with lightweight, high strength and stiffness organic fibers and engineering thermoplastic matrices. Kevlar aramid fibers, for instance, have higher specific tensile strength than glass or carbon fibers, and possess comparable elongation and modulus. These aramid fibers owe their anisotropic properties to highly oriented, rigid molecular chains that are hydrogen bonded in the lateral direction.

The ease of processing thermoplastics makes them an attractive substitute for conventional thermosetting matrices, without sacrificing the tensile and shear properties required to make good composites. Furthermore, the linear chains of thermoforming materials allows unique opportunities to modify the nature of the composite interphase regions. Thus the combination of aramid fiber reinforcing aliphatic polyamides has the potential for an interfacial bond involving matrix crystallization and hydrogen bonding.

It has been shown both in theory and practice that the bulk properties of composites rely heavily on the strength of the interfacial bond and the transfer of load from matrix to fiber via this bond. Compared to the amount of work devoted to the study of interfaces in carbon and glass systems, there is little reported on thermoplastic interface properties with Kevlar. One possible explanation for this lack of information is the complicated fracture mechanisms involved in the failure of this highly anisotropic fiber. Thus, standard short-beam shear tests can give erroneous results for interfacial strength as a result of fiber splitting and poor compressive properties.

A single-filament pull-out test has been previously used to study the interfacial properties of Kevlar-49 in a variety of thermoplastics<sup>1</sup>. Although values for interfacial strengths were obtained, this measurement contains inherent errors due to the small fiber diameter, the radial forces surrounding the fiber (partly the result of differences in thermal expansion coefficients), and the low yield strengths of the matrices. However, single-filament techniques have the advantage of offering a less complicated view of the fiber-matrix interaction. Therefore it was decided to investigate the interfacial properties of Kevlar-aliphatic polyamide composites with measurements of fiber critical length.

CRITICAL LENGTH MEASUREMENTS: Theories and experiments involving short fiber-matrix interactions have been investigated by a number of workers<sup>2-4</sup>. The results show that a fiber, completely embedded in a matrix and loaded in uniaxial tension, experiences a tensile stress due to a load-transfer through the fiber-matrix interface. The load is transferred by shearing stresses at the interface, which reach maximum values near the ends of the discontinuous fiber. As the tensile stress in the fiber builds up to the ultimate fiber strength, it fractures and continues to fail with increased loading of the matrix until there is insufficient transfer of load at the interface. At this point there are three possible mechanisms for failure: (1) the interfacial bond is broken and the fiber becomes uncoupled from the matrix, (2) the yield shear strength of the matrix is exceeded, and/or (3) the fiber itself undergoes a shear failure. Which mode of failure occurs depends on which of the three ultimate shear strengths; bond, matrix, or fiber, is exceeded first. With failure mechanisms (1) and (2), no further fiber tensile fracture occurs and a critical length is obtained. The shear strength calculated using this critical length

is for the interfacial bond or the matrix interfacial yield strength respectively. Measurements of critical lengths have been made with some success to study surface treatments of carbon fibers in epoxy resins<sup>5,6</sup> and the effect of temperature on the bonding between glass fibers and thermosetting matrices<sup>7</sup>.

If the third mode of failure predominates, the fiber will continue to fracture under shear with increased applied tensile loading, resulting in only damaged fiber. This type of failure has not been observed for glass and carbon fibers, but is more likely to occur with an anisotropic fiber due to a presumably much lower shear strength.

Theoretically, all lengths of fiber fragment lengths ( $\ell$ ) formed in a critical length experiment should fall within the range;  $\ell_c/2 \leq \ell \leq \ell_c$ , where  $\ell_c$  is the critical length. Assuming an even distribution of fragment lengths, the critical length can be calculated from<sup>7</sup>

$$\ell_c = \frac{4}{3} \bar{\ell} \quad (1)$$

where  $\bar{\ell}$  is the average fragment length. According to Kelly and Tyson<sup>8,9</sup>, with an elastic fiber in a plastic matrix, the apparent shear strength,  $\tau$ , can be obtained from

$$\tau = \frac{\sigma_f d}{2 \ell_c} \quad (2)$$

where  $d$  is the fiber diameter and  $\sigma_f$  is the ultimate fiber strength. In this paper, samples of single filaments of Kevlar-49 fiber embedded in a nylon-6 film were prepared for investigations of critical lengths, fiber fracture modes, and matrix stress distributions. During sample preparation, shrinkage of the nylon film due to solvent evaporation placed the Kevlar filament under compression. The effect of this compression on fiber properties was also studied.

EXPERIMENTAL

Single filament samples were prepared by solvent casting a nylon-6 film around Kevlar-49 filaments held under slight tension. A 10% (w/w) solution of nylon-6 in 95-97% formic acid was used to cast all films on a glass plate heated to ~70°C. Short lengths of Kevlar yarn (1.5 denier per filament) were first washed in warm methylene chloride to remove any traces of finish, were vacuum dried in an oven at 100°C., and subsequently stored in a dessicator until needed. Cast films containing embedded single fibers were also dried in vacuo at 100°C. and allowed to equilibrate at room temperature and humidity prior to testing. The films were typically 40-50  $\mu\text{m}$  thick. Strips cut from these films were approximately 5 mm wide with a 40 mm gauge length. The strips, with centered fiber, were tensile tested in an Instron at a crosshead rate of 0.05 cm/min. Stretched films were observed under a light microscope with and without crosspolarizers. Fragment lengths and morphologies were studied by a filtration recovery of the fragments after dissolving the matrix with formic acid. The effect of formic acid on the properties of Kevlar is realized. However, it is not expected that any significant changes in the fiber occurs during the relatively short times of exposure to the acid with casting and filtration. Fragment lengths were measured on an optical microscope equipped with a calibrated eyepiece. An ETEC scanning electron microscope was used for investigating fiber surface and fracture morphologies.

RESULTS

(A) COMPRESSION OF KEVLAR: An interesting observation made in the fabrication of samples was the formation of 45° kinks or folds on the fiber surface due to the shrinkage of the nylon during casting. These kinks were formed at compressive strains of  $\leq 2\%$  in a very regular fashion along the entire, continuous fiber length. Previously, workers had noted the formation of these kinked surfaces in: bonding tests<sup>10</sup>, elastica loop tests<sup>11</sup>, and fibers extracted from uniaxially compressed epoxy composites<sup>12</sup>. These kinks can be seen clearly in Fig. 1, which is an SEM photomicrograph of a section of fiber fragment recovered by filtration after tensile deformation of the single filament composite. For comparison, a micrograph of the surface of as-received Kevlar 49 fiber is shown in Fig. 2. It is important to note that the folds can occur as V-shaped bands and not as a single helical crack which might be expected from shear failure of the fiber surface. These kinks were seen to unfold and straighten out when the surrounding film was loaded under tension. Fracture studies of such compressed fibers, allowed to subsequently fail under tension, have shown the failure to occur within a kink band region in a brittle, tensile fashion rather than the fiber splitting mode normally observed with Kevlar<sup>12,13</sup>. However, in this study, most of the fiber fragments (which had been compressed during film casting) recovered for critical length determinations exhibited the splitting into long fibrils at the fracture surface. The reasons for this discrepancy may lie in the fact that the embedded fibers are loaded in shear through the interface at the fiber surface.

Dobb and coworkers<sup>12</sup> found a tensile strength loss associated with the formation of the kinks due to repeated fiber bending over a pulley. The fibers

experience a much more uniform uniaxial compressive strain in the film casting process and therefore provide better samples to investigate the compressive effect on tensile properties. Fibers subjected only to the compressive film shrinkage by application of nylon-6 solutions in formic acid were extracted from the matrix as described above, mounted on cardboard tabs, and tensile tested on an Instron to failure. The results, comparing mechanical properties of these compressed fibers versus as-received fibers of the same gauge length are given in Table 1.

TABLE 1  
Compression Effect by Matrix Casting on Mechanical Properties of  
Kevlar-49 Fiber

<u>Aramid Fiber</u>	<u>Strain to Break</u>	<u>Stress at Break (GPa)</u>	<u>Tensile Modulus (GPa)</u>
As received	2.61 (+0.15)	3.45 (+0.18)	125 (+5.2)
Compressed	2.59 (+0.32)	2.83 (+0.22)	85 (+26.0)

Although there is essentially no change in ultimate elongation, the differences in strength and initial modulus are significant. Fiber compression with kink formation caused a ~20% drop in tensile strength and a reduction in initial modulus that varies widely from sample to sample. A comparison of the stress-strain curves of as-received Kevlar-49 fiber and a typical compressed fiber is given in Fig. 3. The wide variation in moduli for compressed fibers is most likely due to differences in fiber pretension and film shrinkage during the solvent casting process. An interesting observation is that the tangent to the curve of the compressed fibers near break is essentially equal to the

corresponding slope of the curve for untreated fibers with only about 7% variation, irrespective of the initial modulus. This suggests that the kinks can unfold in an almost reversible manner, with chains realigning to regain the modulus lost during compression. The loss of strength, nonetheless, suggests some permanent structural change with kink formation.

B. CRITICAL LENGTH MEASUREMENTS: All single filament "composite" samples were extended to strains greater than 15%. The few films that fractured during stretching were the result of surface defects from sample cutting. Force drops observed on the stress-strain curves, corresponded to fracture events indicating that most fractures occurred within the range of 3-10% strain.

Under a polarizing light microscope, stretched samples showed that the nylon-6 matrix became birefringent around the regions of fiber fracture. This observation indicates the presence of shear stresses, in agreement with the prediction of maximum shearing in the matrix near the fiber ends. Increased elongation of these samples leads to localized necking in these regions suggesting the loss of fiber reinforcement in the fractured fiber sections. The matrix in the immediate vicinity of the non-fractured sections of fiber remains bonded to the fiber and therefore does not exhibit birefringence associated with shearing. These shear stress-free "nodes" are spaced at fairly regular intervals along the fiber.

The fracture lengths were tabulated into three groups of samples: (A) room humidity equilibrated, (B) soaked in distilled water for 2 hours, and (C) soaked for 34 hrs. in water, all at room temperature. The calculated values for  $\bar{x}$ ,  $\ell_c$ , and  $\tau$  are given in Table 2. The error in fragment length measurement is ~10%. The addition of water into the composite was done with the intention of

disrupting any H-bonding at the interface.

TABLE 2

Critical Length Measurements for Kevlar-49 in Nylon-6

<u>Composite History</u>	<u><math>\bar{\ell}</math> (mm)</u>	<u>No. Fragments</u>	<u><math>\ell_c</math> (mm)</u>	<u><math>\tau^*</math> (MPa)</u>
Ambient (A)	2.43 (+0.58)	91	3.24 (+0.77)	5.2 (+1.6)
Water Soaked (2 1/2 hrs.) (B)	1.64 (0.30)	96	2.19 (+0.40)	7.8 (+2.0)
Water Soaked (34 hrs.) (C)	1.95 (+0.43)	89	2.60 (+0.57)	6.5 (+1.9)

\*Based on a compressed fiber tensile strength of 2.83 GPa.

A view of the changes in fracture lengths is given in Fig. 4, the frequency distributions for sample groups (A) and (B). Most values of fragment length fall within the theoretical range of  $1/2\ell_c < \ell < \ell_c$ , with only 3% from group B and 10% from group A being outside their respective limits. These few anomalous lengths can be accounted for by poor wetting or adhesion at parts of the fiber surface and premature failure due to fiber surface defects.

The data suggest an apparent increase in  $\tau$  (i.e. decrease in  $\ell_c$ ) with the addition of water into the system. It is difficult to conceive of water acting to strengthen the bonding at the interface. A more plausible explanation may be suggested by referring to Equation (2). Although not usually considered as such,  $\sigma_f$ , the strength of the fiber, is also a variable in this equation. For a constant  $\tau$ , any decrease in fiber strength would give lower values for  $\ell_c$ . It is well known that water has no effect on the tensile strength of bare Kevlar-49

fiber<sup>14</sup>. The uptake of water by nylons is well known. Nylon-6 can adsorb ~10% (wt.) water at saturation<sup>15</sup>, resulting in a 15% dimensional change<sup>16</sup>. Such swelling of the nylon matrix would place the embedded fiber in axial and radial tension.

The partial unfolding of kinks has been observed in water-soaked samples, indicating some axial tension on the fiber surface. With sufficient swelling, the Kevlar might experience a radial tension that could possibly weaken the fiber. Strong radial tensile forces would act to increase the separation of chains that are only H-bonded laterally. Because the strength of H-bonding decreases with increasing bond distance, weaker interchain interactions would result. Thus, a fiber under radial tension might show a decreased axial tensile strength due to facilitated chain slippage. With lower tensile strength, the continuous fiber would fracture into smaller critical lengths.

An additional complexity is the trend toward larger critical lengths with longer exposure times to water. It may be that after initial rapid swelling of the matrix, there is a slow diffusion of water into the interphase region weakening the bond as first expected. A transcrystalline region of nylon has been seen to form on the fiber surface for films cast under an optical microscope. A tight, crystalline structure would act to inhibit the diffusion of H<sub>2</sub>O into this region. More information is needed to sort out the possible reasons for the water effect on these model Kevlar nylon-6 composites.

It should be noted that values of  $\tau$  and  $l_c$  obtained here cannot be compared directly to other studies on an absolute scale. Because Kevlar fractures with fibrils up to 0.5 mm in length that do not contribute to reinforcement, the relation between measured lengths and critical length differs from glass and carbon fibers where fracture is brittle. Therefore the technique studied in this paper is valid only for relative comparisons with other Kevlar systems.

DISCUSSION AND CONCLUSIONS

Compression of Kevlar-49 fiber was shown to result in an almost reversible kinking at the fiber surface with a corresponding significant loss in strength and modulus. This behavior becomes an important consideration for any Kevlar composite undergoing compressive dimensional changes due, for example, to matrix polymerization, thermal shrinkage, processing, and end-use applications. The results reported here are for one set of casting conditions only. Different results for the fiber compression can be expected with variations in polymer concentration, solvent, evaporation rate, etc.

Critical length measurements resulted in distributions of fragment lengths in close agreement with theory. While values of interfacial shear strength calculated from these measurements are not absolute, the relative changes in distributions indicated that definite variations in interfacial bond strength and/or fiber tensile strength occurred after exposure of the model Kevlar-49 nylon-6 composites to water.

ACKNOWLEDGEMENT

The authors wish to thank E.I. duPont deNemours and Co. for kindly supplying the Kevlar-49 yarn used in this study. Kevlar is a registered trademark of DuPont.

REFERENCES

1. D.B. Eagles, B.F. Blumentritt, and S.L. Cooper, *J. Appl. Polym. Sci.*, 20, 435 (1976).
2. H.L. Cox, *Brit. J. Appl. Phys.*, 3, 72 (1952).
3. D.C. West, *Proceedings, 19th. Annual Conf., SPI, Feb. 1964.*
4. N.F. Dow, G.E. Co., Report R63SD61, 1963.
5. L.T. Drzal, M.J. Rich, J.D. Camping, and W.J. Park, *Proceedings, 35th. Annual Tech. Conf., RP/C, SPI (1980).*
6. L.T. Drzal, M.J. Rich, and P.F. Lloyd, *Polymer Preprints*, 22(2), Section 20-C (1981).
7. T. Ohsawa, A. Nakayama, M. Miwa, and A. Hasegawa, *J. Appl. Polym. Sci.*, 22, 3203 (1978).
8. A. Kelly and W.R. Tyson, *J. Mech. Phys. Solids*, 13, 329 (1965).
9. A. Kelly and W.R. Tyson, *J. Mech. Phys. Solids*, 14, 177 (1966).
10. M.M. Schoppee and J. Skelton, *Textile Res. J.*, P. 968, Dec. 1974.
11. J.H. Greenwood and P.G. Rose, *J. Mat. Sci.*, 9, 1809 (1974).
12. M.G. Dobb, D.J. Johnson, and B.P. Saville, *Polymer*, 22, 960 (1981).
13. R.J. Morgan, E.T. Mones, W.J. Steele, and S.B. Deutscher, *Polymer Preprints*, 21(2) (1980).
14. DuPont Tech. Info., Textile Fibers Dept., Tech. Service Section, Bulletin K-2, Feb. 1978.
15. E.C. Schule in Encyclopedia of Polymer Science and Technology, H.F. Mark and N.G. Gaylord, editors, N.M. Bikales, executive editor, Vol. 10, P. 468, Interscience Publishers, John Wiley & Sons, Inc., N.Y. (1969).

16. E.C. Schule in Encyclopedia of Polymer Science and Technology, H.F. Mark and N.G. Gaylord, editors, N.M. Bikales, executive editor, Vol. 10, P. 467, Interscience Publishers, John Wiley & Sons, Inc., N.Y. (1969).

FIGURE CAPTIONS

- FIGURE 1: Scanning Electron Micrograph of Kevlar-49 Fiber Compressed During Casting of Nylon-6 Film.
- FIGURE 2: Scanning Electron Micrograph of As-Received Kevlar-49 Fiber.
- FIGURE 3: Tensile Stress-Strain Curves of: (A) As-Received Kevlar-49 Fiber, and (B) Kevlar-49 Fiber Compressed During Casting of Nylon-6 Film.
- FIGURE 4: Kevlar-49 Fragment Length Distributions for: (A) Model "Composite" Samples Equilibrated at Ambient Humidity and (B) Model "Composite" Samples Soaked in Distilled Water for 2.5 Hrs. at Room Temperature.



Figure 1

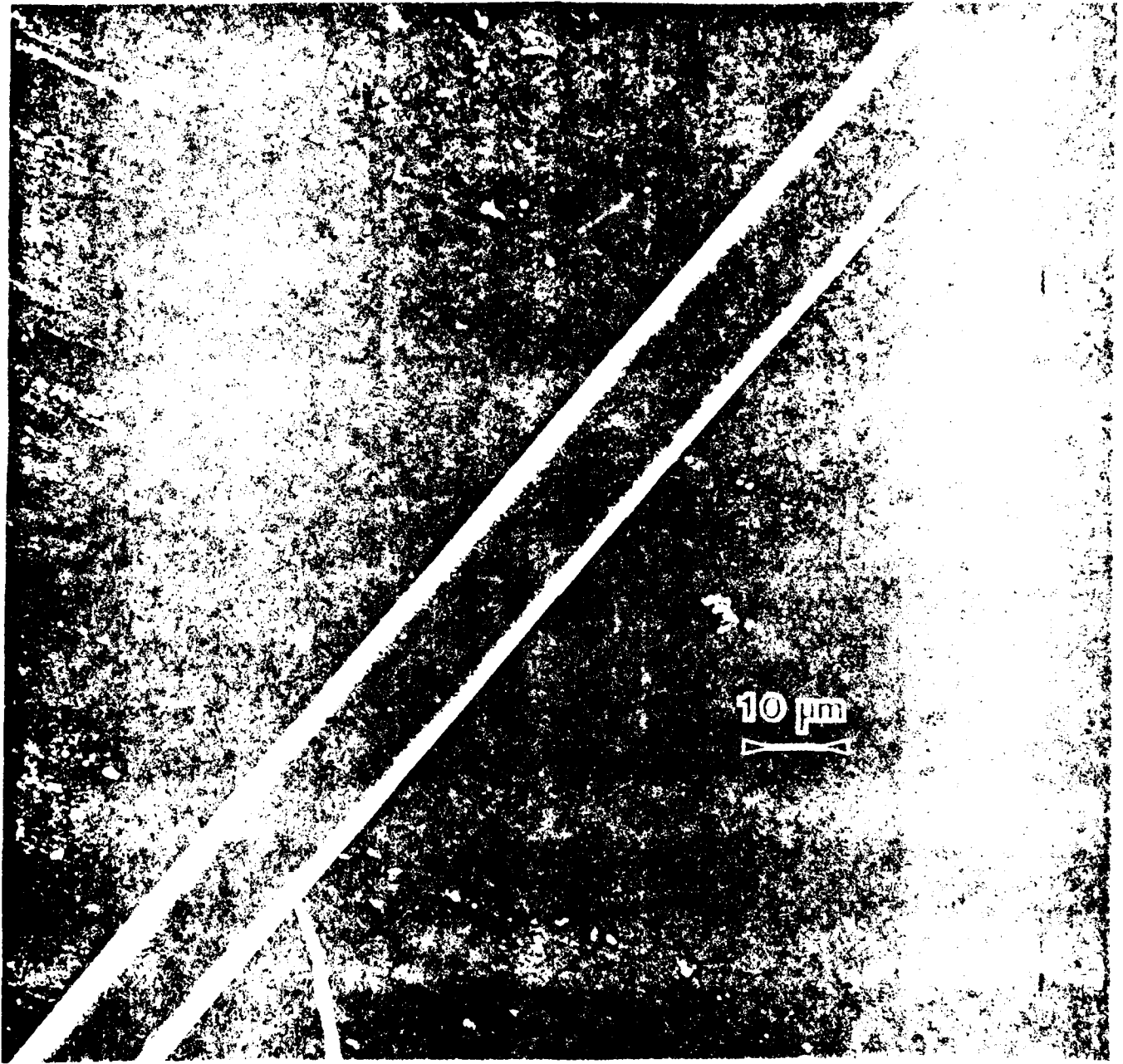


Figure 2

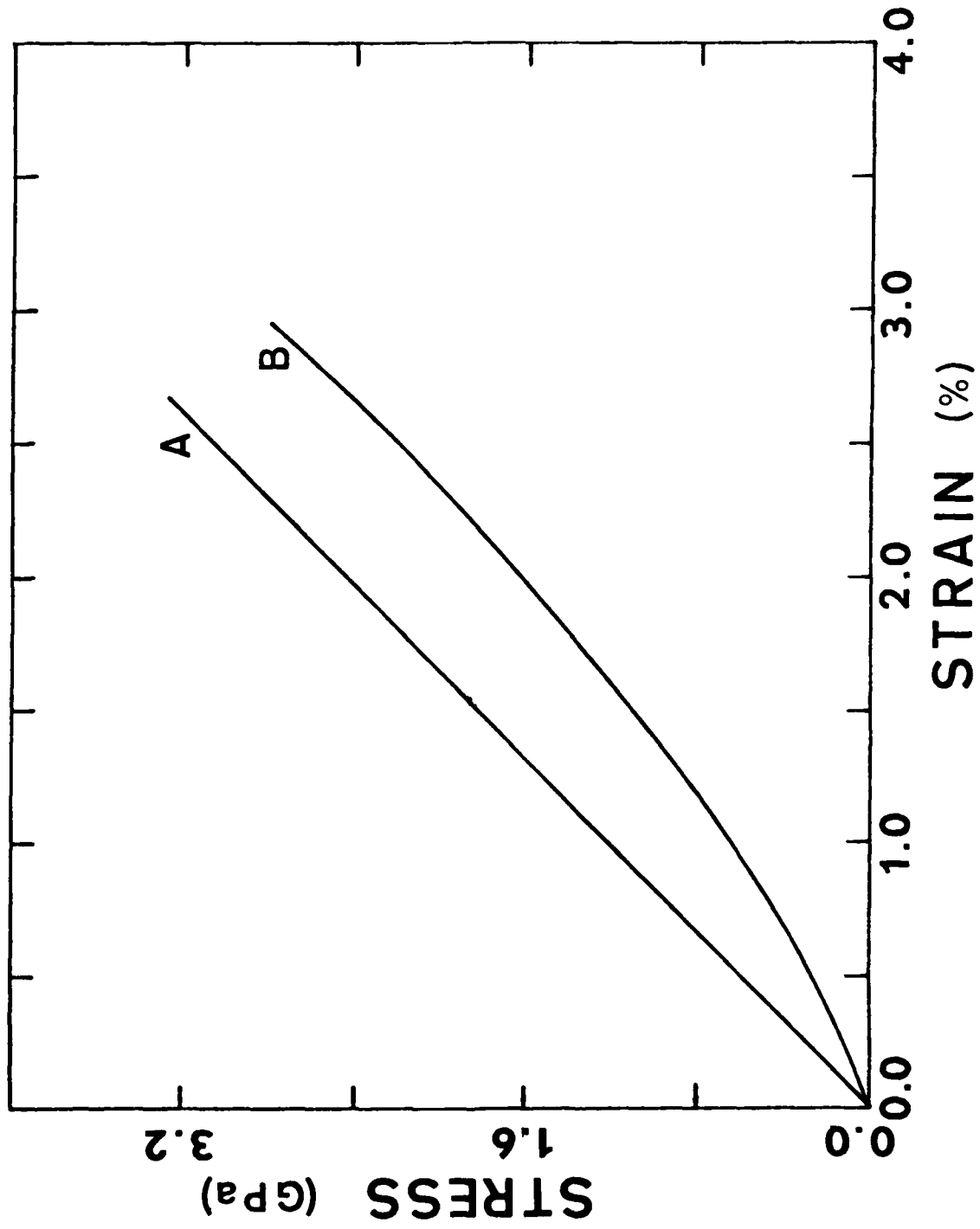


Figure 3

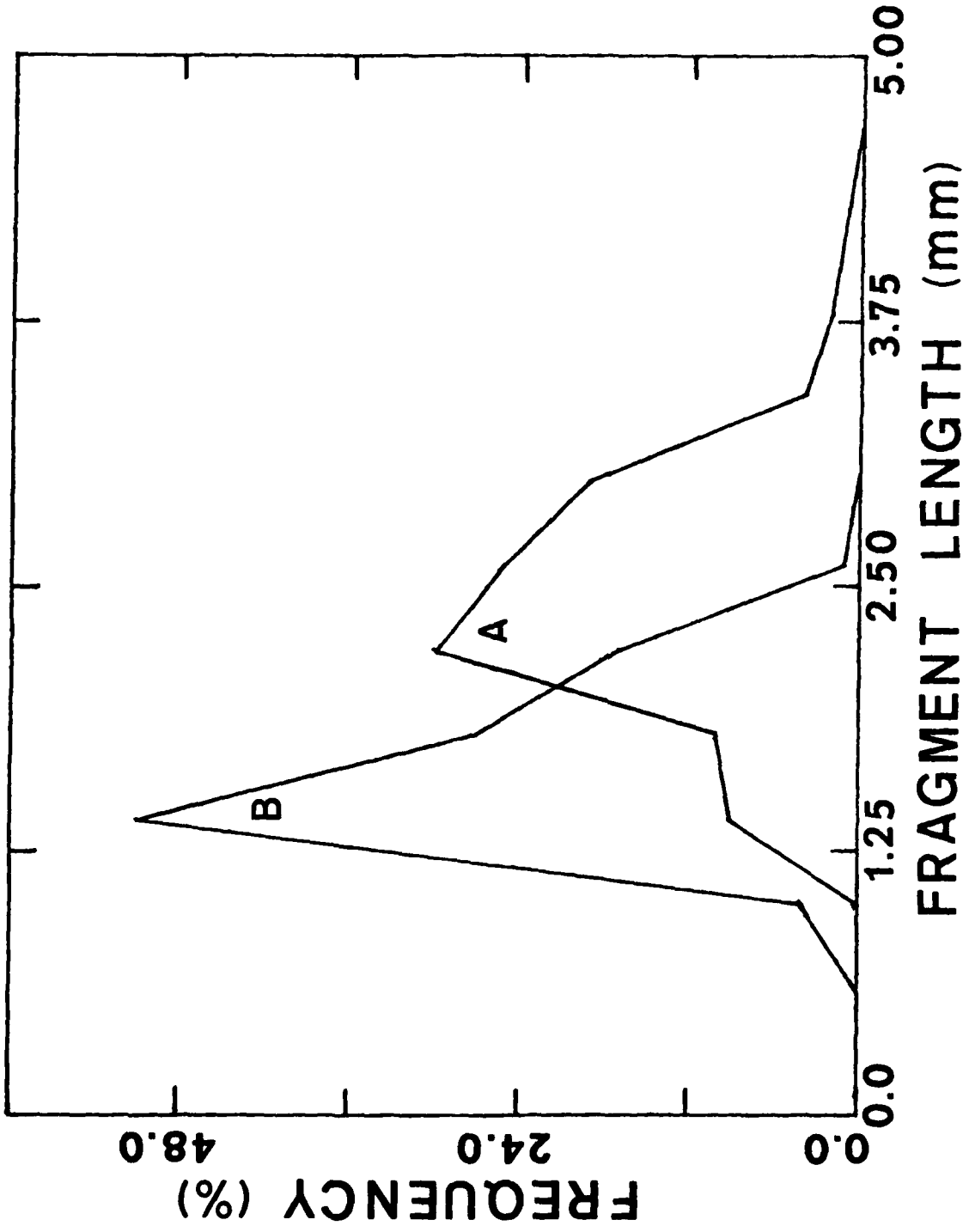


Figure 4

Unclassified

SECURITY CLASSIFICATION OF THIS PAGE (When Data Entered)

REPORT DOCUMENTATION PAGE		READ INSTRUCTIONS BEFORE COMPLETING FORM
1. REPORT NUMBER Technical Report No. 16	2. GOVT ACCESSION NO. AD-4109586	3. RECIPIENT'S CATALOG NUMBER
4. TITLE (and Subtitle) Fracture and Interface Studies of Aramid Reinforced Polyamide Composites: Compressive Effects and Critical Length Measurements	5. TYPE OF REPORT & PERIOD COVERED Interim	
	6. PERFORMING ORG. REPORT NUMBER	
7. AUTHOR(s) Steven J. DeTeresa, Richard J. Farris and Roger S. Porter	8. CONTRACT OR GRANT NUMBER(s) N00014-75-C-0686	
9. PERFORMING ORGANIZATION NAME AND ADDRESS Polymer Science and Engineering University of Massachusetts Amherst, Massachusetts 01003	10. PROGRAM ELEMENT, PROJECT, TASK AREA & WORK UNIT NUMBERS NR 356-584	
11. CONTROLLING OFFICE NAME AND ADDRESS ONR Branch Office 666 Summer Street Boston, Massachusetts 02210	12. REPORT DATE October 20, 1981	
	13. NUMBER OF PAGES 19 (incl. tables and figures)	
14. MONITORING AGENCY NAME & ADDRESS (if different from Controlling Office)	15. SECURITY CLASS. (of this report) Unclassified	
	15a. DECLASSIFICATION/DOWNGRADING SCHEDULE	
16. DISTRIBUTION STATEMENT (of this Report)  Approved for public release; distribution unlimited		
17. DISTRIBUTION STATEMENT (of the abstract entered in Block 20, if different from Report)		
18. SUPPLEMENTARY NOTES		
19. KEY WORDS (Continue on reverse side if necessary and identify by block number)  Fracture, Interface, Aramid, Nylon, Polyamide, Composite, Compression		
20. ABSTRACT (Continue on reverse side if necessary and identify by block number) An investigation of interfacial properties and fiber compression in a class of composites utilizing polymer reinforcement of a polymer matrix was carried out. A model system incorporating single filaments of Kevlar-49 fiber in a nylon-6 matrix was prepared by solution casting the matrix around the fiber. Compression of the fiber caused by shrinkage during the casting process resulted in a fiber surface failure with the formation of kinks at approximately 45° to the fiber axis. Tensile testing of the compressed fibers revealed a decrease in initial tensile modulus and a ~ 20%		

DD FORM 1473  
1 JAN 73

EDITION OF 1 NOV 65 IS OBSOLETE  
S/N 0102-014-6601

Unclassified

SECURITY CLASSIFICATION OF THIS PAGE (When Data Entered)

Unclassified

SECURITY CLASSIFICATION OF THIS PAGE(When Data Entered)

reduction in strength at break. Measured fiber critical lengths fell within the theoretical range in almost every case. Relative changes in fragment length distributions occurred toward smaller critical lengths with exposure of the model composite to water. This suggests an increase in the apparent interfacial shear strength in the presence of water. An explanation for this behavior in terms of variable interfacial shear strength and ultimate fiber strength is proposed. The sensitivity of the properties of the highly anisotropic aramid fiber to composite dimensional changes is realized in both mechanical tests on the bare fiber and critical length measurements.

1

Unclassified

SECURITY CLASSIFICATION OF THIS PAGE(When Data Entered)

TECHNICAL REPORT DISTRIBUTION LIST, GEN

	<u>No.</u> <u>Copies</u>		<u>No.</u> <u>Copies</u>
Office of Naval Research Attn: Code 472 800 North Quincy Street Arlington, Virginia 22217	2	U.S. Army Research Office Attn: CRD-AA-IP P.O. Box 1211 Research Triangle Park, N.C. 27709	1
ONR Branch Office Attn: Dr. George Sandoz 536 S. Clark Street Chicago, Illinois 60605	1	Naval Ocean Systems Center Attn: Mr. Joe McCartney San Diego, California 92152	1
ONR Branch Office Attn: Scientific Dept. 715 Broadway New York, New York 10003	1	Naval Weapons Center Attn: Dr. A. B. Amster, Chemistry Division China Lake, California 93555	1
ONR Branch Office 1030 East Green Street Pasadena, California 91106	1	Naval Civil Engineering Laboratory Attn: Dr. R. W. Drisko Port Hueneme, California 93401	1
ONR Branch Office Attn: Dr. L. H. Peebles Building 114, Section D 666 Summer Street Boston, Massachusetts 02210	1	Department of Physics & Chemistry Naval Postgraduate School Monterey, California 93940	1
Director, Naval Research Laboratory Attn: Code 6100 Washington, D.C. 20390	1	Dr. A. L. Slafkosky Scientific Advisor Commandant of the Marine Corps (Code RD-1) Washington, D.C. 20380	1
The Assistant Secretary of the Navy (R,E&S) Department of the Navy Room 4E736, Pentagon Washington, D.C. 20350	1	Office of Naval Research Attn: Dr. Richard S. Miller 800 N. Quincy Street Arlington, Virginia 22217	1
Commander, Naval Air Systems Command Attn: Code 310C (H. Rosenwasser) Department of the Navy Washington, D.C. 20360	1	Naval Ship Research and Development Center Attn: Dr. G. Bosmajian, Applied Chemistry Division Annapolis, Maryland 21401	1
Defense Documentation Center Building 5, Cameron Station Alexandria, Virginia 22314	12	Naval Ocean Systems Center Attn: Dr. S. Yamamoto, Marine Sciences Division San Diego, California 91232	1
Dr. Fred Saalfeld Chemistry Division Naval Research Laboratory Washington, D.C. 20375	1	Mr. John Boyle Materials Branch Naval Ship Engineering Center Philadelphia, Pennsylvania 19112	1

TECHNICAL REPORT DISTRIBUTION LIST. GENNo.  
Copies

Dr. Rudolph J. Marcus  
Office of Naval Research  
Scientific Liaison Group  
American Embassy  
APO San Francisco 96503 1

Mr. James Kelley  
DTNSRDC Code 2803  
Annapolis, Maryland 21402 1

TECHNICAL REPORT DISTRIBUTION LIST, 356A

	<u>No.</u> <u>Copies</u>		<u>No.</u> <u>Copies</u>
Dr. Stephen H. Carr Department of Materials Science Northwestern University Evanston, Illinois 60201	1	Picatinny Arsenal SMUPA-FR-M-D Dover, New Jersey 07801 Attn: A. M. Anzalone Building 3401	1
Dr. M. Broadhurst Bulk Properties Section National Bureau of Standards U.S. Department of Commerce Washington, D.C. 20234	2	Dr. J. K. Gillham Princeton University Department of Chemistry Princeton, New Jersey 08540	1
Dr. T. A. Litovitz Department of Physics Catholic University of America Washington, D.C. 20017	1	Douglas Aircraft Co. 3855 Lakewood Boulevard Long Beach, California 90846 Attn: Technical Library CI 290/36-84 AUTO-Sutton	1
Professor G. Whitesides Department of Chemistry Massachusetts Institute of Technology Cambridge, Massachusetts 02139	1	Dr. E. Baer Department of Macromolecular Science Case Western Reserve University Cleveland, Ohio 44106	1
Professor J. Wang Department of Chemistry University of Utah Salt Lake City, Utah 84112	1	Dr. K. D. Pae Department of Mechanics and Materials Science Rutgers University New Brunswick, New Jersey 08903	1
Dr. V. Stannett Department of Chemical Engineering North Carolina State University Raleigh, North Carolina 27607	1	NASA-Lewis Research Center 21000 Brookpark Road Cleveland, Ohio 44135 Attn: Dr. T. T. Serofini, MS-49-1	1
Dr. D. R. Uhlmann Department of Metallurgy and Material Science Massachusetts Institute of Technology Cambridge, Massachusetts 02139	1	Dr. Charles H. Sherman, Code TD 121 Naval Underwater Systems Center New London, Connecticut	1
Naval Surface Weapons Center White Oak Silver Spring, Maryland 20910 Attn: Dr. J. M. Augl Dr. B. Hartman	1	Dr. William Risen Department of Chemistry Brown University Providence, Rhode Island 02192	1
Dr. G. Goodman Globe Union Incorporated 5757 North Green Bay Avenue Milwaukee, Wisconsin 53201	1	Dr. Alan Gent Department of Physics University of Akron Akron, Ohio 44304	1

TECHNICAL REPORT DISTRIBUTION LIST, 356A

	<u>No.</u> <u>Copies</u>		<u>No.</u> <u>Copies</u>
Mr. Robert W. Jones Advanced Projects Manager Hughes Aircraft Company Mail Station D 132 Culver City, California 90230	1	Dr. T. J. Reinhart, Jr., Chief Composite and Fibrous Materials Branch Nonmetallic Materials Division Department of the Air Force Air Force Materials Laboratory (AFSC) Wright-Patterson Air Force Base, Ohio 4543	1
Dr. C. Giori IIT Research Institute 10 West 35 Street Chicago, Illinois 60616	1	Dr. J. Lando Department of Macromolecular Science Case Western Reserve University Cleveland, Ohio 44106	
Dr. M. Litt Department of Macromolecular Science Case Western Reserve University Cleveland, Ohio 44106	1	Dr. J. White Chemical and Metallurgical Engineering University of Tennessee Knoxville, Tennessee 37916	
Dr. R. S. Roe Department of of Materials Science and Metallurgical Engineering University of Cincinnati Cincinnati, Ohio 45221	1	Dr. J. A. Manson Materials Research Center Lehigh University Bethlehem, Pennsylvania 18015	1
Dr. Robert E. Cohen Chemical Engineering Department Massachusetts Institute of Technology Cambridge, Massachusetts 02139	1	Dr. R. F. Helmreich Contract RD&E Dow Chemical Co. Midland, Michigan 48640	1
Dr. David Roylance Department of Materials Science and Engineering Massachusetts Institute of Technology Cambridge, Massachusetts 02039	1		
Dr. T. P. Conlon, Jr., Code 3622 Sandia Laboratories Sandia Corporation Albuquerque, New Mexico	1	Professor Garth Wilkes Department of Chemical Engineering Virginia Polytechnic Institute and State University Blacksburg, Virginia 24061	1
Dr. Martin Kaufmann, Head Materials Research Branch, Code 4542 Naval Weapons Center China Lake, California 93555	1	Dr. Kurt Baum Fluorochem Inc. 6233 North Irwindale Avenue Azusa, California 91702	1
Professor S. Senturia Department of Electrical Engineering Massachusetts Institute of Technology Cambridge, Massachusetts 02139	1	Professor C. S. Paik Sung Department of Materials Sciences and Engineering Room 8-109 Massachusetts Institute of Technology Cambridge, Massachusetts 02139	1

DATE  
FILME

2-8